Quantum chemical study of reaction mechanism between plutonium and Nitrogen

Zhao-Yang Zhao (zzy13474295519@sina.com)
PLA Rocket Force University of Engineering https://orcid.org/0000-0002-0914-1956
Guo-Liang Wang
PLA Rocket Force University of Engineering
Xu-Dan Chen
PLA Rocket Force University of Engineering
Chun-Bao Qi
PLA Rocket Force University of Engineering
Xin-Li Sun
PLA Rocket Force University of Engineering

Research Article

Keywords: Plutonium, Reaction mechanism, Density functional theory, Reaction rate constant, Nitride

Posted Date: June 24th, 2021

DOI: https://doi.org/10.21203/rs.3.rs-647666/v1

Quantum chemical study of reaction mechanism between plutonium and Nitrogen

Zhao-Yang Zhao[1], Guo-Liang Wang[2], Xu-Dan Chen[1], Chun-Bao Qi[1], Xin-Li Sun[2]

Zhao-Yang Zhao1, (*)
Graduate School, Rocket Force University of Engineering,
Xian, Shanxi, 710025 People's Republic of China
E-mail:zzy13474295519sina.com

Guo-Liang Wang2,
Nuclear Science and Technology Laboratory, Rocket Force University of Engineering,
Xian, Shanxi, 710025 People's Republic of China
E-mail:wgl_728@aliyun.com

Xu-Dan Chen1,
Graduate School, Rocket Force University of Engineering,
Xian, Shanxi, 710025 People's Republic of China
E-mail:nuaamk@163.com

Chun-Bao Qi1,
Graduate School, Rocket Force University of Engineering,
Xian, Shanxi, 710025 People's Republic of China
E-mail:qazwsx4060@126.com

Xin-Li Sun2,
Nuclear Science and Technology Laboratory, Rocket Force University of Engineering,
Xian, Shanxi, 710025 People's Republic of China
E-mail:s_xinl@sina.com

Abstract

The study of the reaction between plutonium and nitrogen is helpful to further understand the interaction between plutonium and air gas molecules. For the nitridation reaction of plutonium, there is no report on the microscopic reaction mechanism of this system at present. Therefore, the microcospic mechanism of gas phase reaction of Pu with N_2 is studied in this paper based on the density functional theory (DFT) using different functions. In this paper, the geometry of stationary points on the potential energy surface is optimized. In addition, the transition states are verified by the frequency analysis method and the intrinsic reaction coordinate (IRC) method. Finally, we obtain the reaction potential energy curve and the micro reaction pathways. The analysis of reaction mechanism shows that the reaction of Pu with N_2 has two pathways. The pathway-1 ($Pu+N_2 \rightarrow R1 \rightarrow TS1 \rightarrow PuN_2$) has a T-shaped transition state and the pathway-2 ($Pu+N_2 \rightarrow R_2 \rightarrow TS_2 \rightarrow PuN+N$) has a L-shaped transition state. Moreover, both transition states have only one virtual frequency. The energy analysis shows that pathway-1 is the main reaction pathway. The nature of the Pu-N bonding evolution along the pathways is studied by atoms in molecules (AIM) and electron localization function (ELF) topological approaches. In order to analyse the role of 5f orbital of plutonium atom in the reaction, the variation of density of state along the pathways is performed. The results show that the 5f orbital makes major contributions to the formation of Pu-N bonds. Meanwhile, the influence of different temperatures on the reaction rate is revealed by calculating the rate constants of the two reaction pathways.

Keywords: Plutonium; Reaction mechanism; Density functional theory; Reaction rate constant; Nitride

Introduction

The gas phase of actinide elements study can reveal a lot of reaction details which are difficult to obtain by experiments. General references for this problem can be found in many papers [1-7]. Plutonium is a complex actinide element, which has wide applications in the field of energy. It locates at the boundary between the light actinide elements containing delocalized 5f electrons and the heavy actinide elements containing localized 5f electrons. This particular electron structure [8] endows it some complex physical and chemical properties [9,10]. When exposed to air, plutonium can react with oxygen, nitrogen, water and hydrogen easily to form a variety of compounds which will cause surface oxidation and corrosion. These phenomena have a great impact on the usage and storage of plutonium, and have become a research focus in recent years. A large number of studies on the interaction between actinides and small gas molecules have provided theoretical and experimental basis for the study of solving this problem. However, due to the high toxicity and radioactivity of plutonium, the basic scientific research of plutonium still faces many challenges. Therefore, it is necessary to study the reaction mechanism of corrosion process from microscopic point of view. In recent years, there are scholars have done quantum chemical calculations on the detailed reaction mechanism of gas actinides atoms and gas small molecules, including $Pu+O_2$ [11], $U^+(U^{2+})+H_2O$ [12], $Pu+H_2O$ [13], etc. They obtained multiple reaction pathways of these reactions and the geometric structures of each stationary point along the reaction pathway. Some scholars have also conducted theoretical and experimental studies on the interaction between small gas molecules and plutonium solid surface. Experimentally, the kinetics of reaction of plutonium with oxygen, water and moist air has been studied in the literature [14-16], and the mechanism of water-catalyzed oxidation has been proposed. In terms of theoretical calculation, some scholars [17] used density functional method to simulate the interaction between C, N and O atoms and plutonium surface. However, there is no research on the microscopic reaction mechanism between plutonium atoms and nitrogen molecules at present.

The main work of this paper is to study the microscopic reaction mechanism of plutonium atom in gas phase and nitrogen molecule by simulation. Two reaction pathways have been found and the geometric structures of all equilibrium and transition states in the reaction pathways have been optimized and demonstrated. The electron localization function (ELF) [18-20] and the atoms in molecules (AIM) [21-23] theoretical method are used to analyze the bond evolution process. By calculating the density of state of each stationary structure, the role of 5f orbital of plutonium atom in the bonding process is compared and analyzed. Furthermore, by calculating the reaction rate constants of the two reaction pathways at different temperatures, the reaction rates of plutonium and nitrogen along the two pathways at different temperatures are discussed.

Theoretical Calculation Methods

All the theoretical calculations involved in this paper are based on the density functional theory (DFT) using the Gaussian 16 program package [24]. We adopt the hybrid functional method B3LYP [25,26], which not only coupled the Becke switching functional with gradient correction and Lee, Yang and Parr correlation functional with gradient correction, but also processed its local correlation functional with Vosko, Wilk and Nusair (NWN) local spin density. In previous calculations , the B3LYP method demonstrates the advantages in handling strongly associated systems, especially, when calculating the reaction between plutonium atoms and small molecules of common gases in the air, the calculated results with this function match the experimental data best [27]. For the structural optimization of each equilibrium state and transition state, nitrogen atoms adopt the polarization basis set 6-31g(d,p), and plutonium adopts the Stuttgart small nucleus relativistic effective pseudopotential [28] (SDD), which replaces the 60 electrons in shells 1-4, leaving the $n \geq 5$ shells as valence electrons. For accurate calculation of single point energy and vibration frequency of the optimized structure, nitrogen atoms are calculated by def2-TZVP, a high angular momentum basis set, while plutonium atom is still calculated by SDD basis set.

By analyzing the energy and vibration frequency, we confirm whether the equilibrium structure is located

at the minimum point and whether the transition state structure has only one virtual frequency. Meanwhile, the intrinsic reaction coordinate (IRC) are calculated to verify whether the transition state structure is connected to the two minimum points. Since the spin-orbit interaction has little effect on the molecular structure of actinides [29,30], the spin-orbit effect is not considered in all calculations in this paper.

AIM theoretical analysis of chemical bonds mainly relies on topological analysis to find the most representative bond critical point [31] (bcp) in the interatomic interaction region, whose properties can be used to investigate the characteristics of the corresponding chemical bonds such as strength and nature [32-35]. It is generally believed that the greater the electron density $\rho(r)$ at the position of bcp and the smaller the electron potential energy density V(r), the greater the strength of homogenous bonds, and that the corresponding bond can be considered covalent if the Laplace function of the electron density $\nabla^2\rho(r)$ is negative [36,37]. The values of $|V(r)|/G(r)$ ($H(r)=G(r)+V(r)$, G(r) is the kinetic energy density of electrons) and $H(r)/\rho(r)$ can also be used to determine the type of interaction between the corresponding two atoms [38]. The ELF shaded surface projection map for each equilibrium state and transition state can show the bond evolution process more intuitively, and the selection of basis sets will not affect the ELF analysis results. The density of state (DOS) figure is useful for analyzing the structural characteristics of chemical systems. By calculating the partial DOS (PDOS) of 5f orbital of each equilibrium and transition state structure and comparing them with the total DOS (TDOS) of the structure and the overlap population DOS (OPDOS) of the interaction between plutonium atom and nitrogen atoms, the contribution of 5f orbital of plutonium atoms to the bond evolution process can be obtained. All the above calculations are performed by the Multiwfn program.

Based on the transition state theory (TST) [37] and the methods and steps of calculation proposed by Dr. Sobereva [36], we calculate the reaction rate constants of the two reaction pathways at different temperatures, and use them to investigate the reaction rates in the temperature range of 273.15 K~2273.15 K. It is worth emphasizing that the thermodynamic data needed for calculation are obtained by Shermo program [39].

Results and Discussion

Reaction mechanisms

There are two different reaction pathways for $Pu+N_2$ reaction, pathway-1: $Pu+N_2 \rightarrow R1 \rightarrow TS1 \rightarrow PuN_2$, pathway-2: $Pu+N_2 \rightarrow R2 \rightarrow TS2 \rightarrow PuN+N$. The geometric structures and relative energies of all the equilibrium and transition states in the two pathways are shown in Fig. 1 and Fig. 2, respectively. As shown in Fig. 1, for pathway-1, plutonium atom approach nitrogen molecule from the direction perpendicular to the N2-N3 bond, forming the initial reactant R1. For pathway-2, the plutonium atom approaches the nitrogen molecule from a direction parallel to the N2-N3 bond, forming the initial reactant R2, whose three atoms are approximately collinear. By analyzing the data in Table 1, it can be seen that the bond length of the N2-N3 bond in R1 is 0.13163 Å, which is longer than that of the N2-N3 bond in R2. Moreover, as shown in Fig.2, the energy of R1 is higher than that of R2, indicating that R2 is more stable than R1. This indicates that plutonium atom and nitrogen molecule are more likely to be activated when they are close to each other perpendicularly to the N2-N3 bond and to separate the two nitrogen atoms in the nitrogen molecule. Similarly, as shown in Fig.1, Fig.2 and Table 1, in pathway-1, when the system passes a 109.4 kJ/mol barrier from R1 to product PuN2, the length of Pu1-N2 and Pu1-N3 bonds gradually becomes shorter, and the distance between two nitrogen atoms gradually increases, and the N2-N3 bond in transition state TS1 has been completely broken.

Fig.1 The optimized geometric structure diagram of all intermediates and transition states

In addition, for pathway-2, from R2 to product PuN+N, the system passes through a barrier as high as 365.7 kJ/mol, and the length of the Pu1-N2 bond gets shorter and shorter, and the length of the N2-N3 bond gets longer and eventually breaks completely. The TS1 and TS2 have only one virtual frequency, which verifies the rationality of the structure. By analyzing the structural parameters of TS1 and TS2 and the vibration patterns corresponding to their virtual frequency, it can be seen that the plutonium atom and

the two nitrogen atoms in pathway-1 have the tendency to form bond, and the two nitrogen atoms have the tendency to separate gradually. The plutonium atom in pathway-2 tends to form bond with the nitrogen atom close to it, and the two nitrogen atoms also tend to separate gradually.

Fig.2 The relative energies of all intermediates and transition states involved in the two reaction pathways composites

In general, the barrier of reaction pathway-2 is significantly higher than that of reaction pathway-1. The energy of products in reaction pathway-2 is 341.8 kJ/mol, which is higher than that of its reactant, while the energy of product in reaction pathway-1 is 237.9 kJ/mol, which is lower than that of its reactants. And the energy of the transition state in pathway-1 is much lower than in pathway-2. These phenomena indicate that pathway-1 is more likely to occur than pathway-2. The two pathways both happen along the triplet spin surface. It is worth noting that, as you can see, the reaction mechanism of $Pu+N_2$ is similar to that of $Pu+O_2$[11] and $Pu+H_2O$[13] , plutonium atoms interact with gas molecules to dissociate them, and the atoms after dissociation form bonds with plutonium atoms.

For pathway-1, it can be found from Table 2 that there is a (3, -1) bcp between plutonium atom and each nitrogen atom in R1, TS1 and PuN2 molecules. In addition, the topological properties of the two bcps are identical. Fig.3 shows the consistency of Pu1-N2 interaction and Pu1-N3 interaction in the reaction process can also be obtained. These phenomena indicate that the interaction between the plutonium atom and the two nitrogen atoms is completely synchronous along reaction pathway-1. For the R1 structure, The $\nabla 2\rho(r)$ [40,41] at the bcps between plutonium and nitrogen atoms is positive, the values of V(r) and H(r)/ ρ (r) are negative, and the value of |V(r)|/G(r) is greater than 1 and less than 2. Combined with the previous studies [41,40,42,43], we can conclude that these phenomena indicate that the interaction between plutonium atom and nitrogen atom is closed-shell interaction with covalent character. Similarly, the interaction between plutonium atom and nitrogen atom in TS1 is also a closed-shell interaction with stronger covalency. However, the interaction between plutonium atoms and nitrogen atoms in PuN_2 molecule is a thoroughly covalent interaction. By analyzing the parameters of bcp between two nitrogen atoms in R1, we can see that the values of $\nabla^2\rho(r)$, H(r), and H(r)/ρ(r) are all much less than 0, and the values of |V(r)|/G(r) are greater than 2. These phenomena indicate that the N1-N2 bond in R1 is a strong covalent bond. However, there was no bcp between the two nitrogen atoms in the TS1 and PuN_2 molecules, indicating that the N1-N2 bond was completely broken during the process from R1 to TS1. This view is also supported by a marked decrease in electron localization between the two nitrogen atoms as seen in the ELF projection map of TS1. Through a comprehensive analysis of the data in table 2, we find that the properties of the bcps between the plutonium atom and the two nitrogen atoms has changed greatly during the reaction, specifically for, the value of ρ(r) increases gradually, the values of V(r), H(r) and H(r)/ρ(r) are less than 0 and gradually decrease, and the value of $\nabla^2\rho(r)$ has changed from positive to negative, the value of |V(r)|/G(r) increases gradually and eventually it gets bigger than 2. Based on these changes, we believe that the interaction between plutonium atoms and the two nitrogen atoms gradually increases and changes from the initial closed shell interaction to covalent interaction, that is, the two Pu-N bonds in the product PuN_2 molecule are covalent bonds. It can also be clearly seen from the ELF projection map that with the progress of the reaction, the degree of electron localization between plutonium atom and two nitrogen atoms gradually increases, and two nitrogen atoms in PuN_2 molecule, the product, have separated on both sides of plutonium atom, and there are two synaptic valence basons between Pu1-N2 bond and Pu1-N3 bond, respectively.

By using the same method to analyze the data of reaction pathway-2 in Table 2, it can be obtained that the values of $\nabla^2\rho(r)$, H(r) and H(r)/ρ(r) of bcp between two nitrogen atoms in R2 are negative and their absolute values are relatively large, while the value of |V(r)|/G(r) is positive and greater than 2. Thus, we can conclude that the N2-N3 bond in R2 is a strong covalent bond and stronger than the N2-N3 bond in R1, which also indicates that plutonium atoms are more likely to activate and break the N2-N3 bond when they approach nitrogen molecules from the direction perpendicular to the N2-N3 bond. Since the values of $\nabla^2\rho(r)$, H(r), and H(r)/ρ(r) of bcp between atom Pu1 and atom N2 in R2 are positive, we can consider the interaction between these two atoms as the closed shell interaction, and since the value of ρ(r) and the absolute value of

V(r) of bcp are relatively small, the interaction is weak. The absolute values of ρ(r) and V(r) at the bcp between two

Table 1 The partial geometric structure parameters of all intermediates and transition states and the vibration frequencies of their different vibration modes

		R1	TS1	PuN2	R2	TS2	PuN+N
Bond distances/Å	Pu1-N2	2.16422	1.84003	1.70983	2.45311	1.77304	1.76172
	Pu1-N3	2.16422	1.84003	1.70983	-	-	-
	N2-N3	1.24866	1.84071	3.41966	1.11703	2.11771	3.03429
Vibration frequency/cm-1	Mode 1	442.68	-420.98	209.65	105.30	-1489.05	23.65
	Mode 2	500.49	651.05	1002.51	154.50	90.18	55.28
	Mode 3	1389.72	837.27	1068.52	2043.30	552.29	814.38

Bond evolution analysis

Table 2 Topological properties of the charge density calculated at the (3, -1) bcps for all species involved in the reaction pathways

Structure	Species	ρ(r)/a.u.	∇2ρ(r)/a.u.	G(r)/a.u.	V(r)/a.u.	H(r)/a.u.	|V(r)|/G(r)	H(r)/ρ(r)
R1	Pu1-N2	0.1275878	0.2463471	0.1098352	-0.1580857	-0.0482505	1.4392990	-0.3781750
	Pu1-N3	0.1275878	0.2463471	0.1098352	-0.1580857	-0.0482505	1.4392990	-0.3781750
	N2-N3	0.4752959	-1.2167513	0.3312256	-0.9666389	-0.6354134	2.9183706	-1.3368794
TS1	Pu1-N2	0.2690981	0.2725819	0.2791655	-0.4901992	-0.2110337	1.7559448	-0.7842261
	Pu1-N3	0.2690981	0.2725819	0.2791655	-0.4901992	-0.2110337	1.7559448	-0.7842261
PuN2	Pu1-N2	0.3754259	-0.0884678	0.3855768	-0.7932945	-0.4077178	2.0574228	-1.0860139
	Pu1-N3	0.3754259	-0.0884678	0.3855768	-0.7932945	-0.4077178	2.0574228	-1.0860139
R2	Pu1-N2	0.0534947	0.2230454	0.0597905	-0.0638201	0.0040296	1.0673946	0.0753262
	N2-N3	0.6652988	-2.4786016	0.5540964	-1.7278432	-1.1737468	3.1183079	-1.7642399
TS2	Pu1-N2	0.3093716	0.1687179	0.3261208	-0.6100791	-0.2839582	1.8707148	-0.9178549
	N2-N3	0.0575919	0.1653797	0.0430595	-0.0447741	-0.0017146	1.0398188	-0.0297712
PuN+N	Pu1-N2	0.3213386	0.1318760	0.3371840	-0.6414168	-0.3042328	1.9022754	-0.9467672
	N2-N3	0.0078971	0.0267055	0.0054495	-0.0042226	0.0012269	0.7748588	0.1553618

nitrogen atoms in TS2 are very small, and thus we can assume that the interaction between the two nitrogen atoms is extremely weak, and the N2-N3 bond has been completely broken. However, the values of H(r) and H(r)/ρ(r) for bcp between atom Pu1 and atom N2 are negative, the values of |V(r)|/G(r) are approximately 2, and the absolute values of ρ(r) and V(r) are much larger than that of R2. These phenomena indicate that the Pu1-N2 interaction in TS2 is much stronger than that in R2. It is converted to covalent interaction. Based on the same method, the AIM analysis of the product structure of reaction pathway-2 shows that the covalent interaction between Pu1-N2 is stronger than that of TS2, so that the covalent bond between Pu1 and N2 can be considered to be formed in the product. In general, as the reaction progresses, the interaction between N2 and N3 gradually weakens, while the interaction between Pu1 and N2 gradually becomes strong and forms a covalent bond. As can be seen from the ELF projection map of R2 in Fig.3, there is no valence basin between plutonium atom and nitrogen atom, while there is a bisynaptic valence basin between the two nitrogen atoms. When TS2 is formed, there is no valence basin between the two nitrogen atoms, which indicates that the N2-N3 bond has been broken and the interaction between Pu1 and N2 is greatly enhanced. As can be seen from the ELF projection map of the product, a valence basin is formed between Pu1 and N2 and the interaction between the two nitrogen atoms is further weakened. This is consistent with the analysis results of AIM.

Fig. 3 ELF projection map of all intermediates and transition states

Density of states

As shown in Fig.4, the black curve represents DOS, the red curve represents the PDOS for the 5f orbital of Pu1 atom, and the blue curve represents the PDOS for the two nitrogen atoms. The green OPDOS curve examines whether molecular orbitals in different energy regions are bonding or anti-bonding or have little or no effect on Pu1 atom and nitrogen atoms. Tian Lu' s study[36] indicates that if the OPDOS curve of a certain region is significantly positive, it means that the molecular orbital of this energy region has a promoting effect on the combination of two segments, which will play a bonding effect. If it is significantly negative, it means that the molecular orbital of this energy region is unfavorable to the combination and will have anti-bonding effect; if the value is close to 0, the effect on the combination is relatively small. The dotted lines show the HOMO (Highest Occupied Molecular Orbital) positions, and the contours of the HOMO of the stationary points are also shown in this figure.

By analyzing the density of states of R1, TS1 and PuN_2 molecule in pathway-1, it can be found that in R1, the orbitals with energy lower than -0.28 a.u. are basically contributed by the orbitals of two nitrogen atoms, while those with energy higher than -0.28 a.u. are mainly contributed by the 5f orbital of plutonium atom and the orbitals of two nitrogen atoms. On the HOMO position, the PDOS of plutonium atom' s 5f orbital is very close to TDOS, indicating that the HOMO is mainly composed of plutonium atom' s 5f orbital, and the participation of two nitrogen atoms is weak. Moreover, the OPDOS curve at the HOMO position is positive, which indicates that the interaction between the 5f orbital of plutonium at the HOMO position of R1 and two nitrogen atoms can promote the formation of Pu-N bond. In TS1, the orbitals with energy that is lower than -0.52 a.u. are basically contributed by the orbitals of two nitrogen atoms, while those with energy higher than -0.39 a.u. are mainly contributed by the 5f orbital of plutonium atom and the orbitals of two nitrogen atoms. The OPDOS curve is clearly positive in the range that contains the HOMO energy. Moreover, the density of state of the 5f orbital of plutonium atom and the orbital of two nitrogen atoms peaks, which indicates that the interaction between the 5f orbital of plutonium atom and the orbital of two nitrogen atoms also promotes the formation of Pu-N bond. The degree of promotion is much greater than that in R1. In the product PuN_2 molecule, similarly, the TDOS in the low energy region is mainly contributed by the orbitals of two nitrogen atoms, while the TDOS in the high energy region is mainly contributed by the 5f orbital of plutonium and the orbitals of two nitrogen atoms. The degree of promotion is much greater than that in R1. In the product PuN_2 molecule, similarly, the TDOS in the low energy region is mainly contributed by the orbitals of two nitrogen atoms, while the TDOS in the high energy region is mainly contributed by the 5f orbital of plutonium and the orbitals of two nitrogen atoms. In general, the 5f orbital of plutonium atom makes a major contribution to the formation of Pu-N bond. As the reaction progresses along reaction pathway-1, the tendency of plutonium atom and two nitrogen atoms to form chemical bonds is increasing, and the effect of nitrogen atoms on the

formation of chemical bonds gradually increases.

Fig.4 The TDOS, PDOS and OPDOS for all intermediates and transition states.

In the following, we will discuss the electronic density of states of R2, TS2 and PuN+N structure in reaction pathway-2. It can be concluded that TDOS in low energy region is basically contributed by the orbitals of two nitrogen atoms, while TDOS in high energy region is contributed by the 5f orbital of plutonium and the orbitals of two nitrogen atoms. In TS2, the OPDOS curve in the energy range of -0.31 a.u~-0.19 a.u. is positive and has the highest peak value. Thus, the interaction between the 5f orbital of plutonium atom and two nitrogen atom orbitals in this energy range strongly promotes the formation of Pu-N bond. In the product (PuN+N) structure, similarly, the OPDOS curve is positive in the energy range of -0.33 a.u.~-0.22 a.u., and the interaction between 5f orbital of plutonium and two nitrogen atom orbitals is also bonding interaction. Generally speaking, consistent with reaction pathway-1, the 5f orbital of plutonium atom contributes more to the formation of Pu-N bond than the orbitals of two nitrogen atoms. Through comprehensive analysis of all the structures shown in Fig.4, we found that the 5f electron of plutonium atom played a important role in the formation of Pu-N bond, and the role of two nitrogen atoms gradually increased. Therefore, it can be said that the formation of Pu-N bond is mainly caused by the interaction between 5f electron of plutonium atom and two nitrogen atoms. This phenomenon is similar to the formation of Pu-O bond in the reaction of plutonium and oxygen[11].

Kinetic analysis

As shown in Fig.5, by investigating the reaction rate constant at different temperatures at 1 atm (standard atmospheric pressure, 101.325 kPa), we can conclude that the reaction rate constant k1 is 1.67E-07 $s^{-1}mol^{-1}$ at 273.15 K, 1.06E-05 $s^{-1}mol^{-1}$ at 298.15 K, but increases to 7.49E+12 $s^{-1}mol^{-1}$ at 2273.15 K. These results indicate that the reaction of R1→PuN_2 can be carried out at low temperature and the reaction rate increases with the increase of temperature. For the reaction R2→PuN+N, it can be found that, with the change of temperature from 273.15 K to 523.15 K, the rate constant k2 changes from 2.69E-55 $s^{-1}mol^{-1}$ to 1.13E-22 $s^{-1}mol^{-1}$, which indicates that the reaction will not happen in the temperature range of 273.15 K to 523.15 K, but with the increasement of temperature, the reaction rate constant will also gradually become very large. For example, when the temperature rises to 2273.15 K, k2 increases to 8.45E+06 $s^{-1}mol^{-1}$.

Fig.5 The reaction rate constant (k) of R1→PuN_2 and R2→PuN+N in the temperature range of 273.15K-2273.15K (the pressure is set at 1atm).

It can be intuitively seen from Fig.5 that R1→PuN_2 is easy to go forward in the range of 273.15 K-2273.15 K, while R2→PuN+N is relatively difficult. It is worth noting that, with the increase of temperature, the increasing speed of reaction rate constant k gradually slows down, which indicates that the reaction rate constant is greatly influenced by temperature at low temperature, while the influence degree on reaction rate constant gradually decreases with the increase of temperature. The results show that N_2 in the air will also participate in plutonium corrosion in the temperature range of 273.15 K-2273.15 K. If the interaction of other gases is not considered, the main product of plutonium nitriding corrosion is PuN_2.

Conclusions

In this paper, the gas phase reaction of plutonium and nitrogen is studied by DFT method. The results show the microscopic reaction mechanism of this reaction in detail. When the spin multiplicity of the system is set to triplet, two reaction pathways are found. In addition, the structure of each stationary point in the reaction pathways has been optimized. At the same time, we obtain the energy of each stationary point and analyze the

change of energy along the reaction pathways. For the evolution process of bonds, we use two different topological analysis methods (ELF and AIM) to analyse the changes of electronic properties at bcps. Furthermore, in order to investigate the contribution of the interaction between the 5f orbital of plutonium atom and the orbitals of two nitrogen atoms in the formation of Pu-N bond, we analyze the density of states of each stationary point. In addition, in order to figure out the reaction rate of each reaction pathway at different temperatures, we calculate reaction rate constant (k) of each reaction pathway at different temperatures by Shermo program [38] and transition state theory (TST) [37]. All analysis results are shown below.

1) Plutonium atoms and nitrogen molecules approach each other in different ways to form the initial complexes (R1 and R2) with different structures, and two different reaction pathways are generated as the reaction progresses.

pathway-1: $Pu+N_2 \rightarrow R1 \rightarrow TS1 \rightarrow PuN_2$

pathway-2: $Pu+N_2 \rightarrow R2 \rightarrow TS2 \rightarrow PuN+N$

2) The results of energy analysis and kinetics analysis of each structure in the two reaction pathways show that reaction pathway-1 is more likely to occur than reaction pathway-2. At the same temperature, there is a great difference in reaction rates between them. Through the results， we can conclude that N_2 in the air will also participate in plutonium corrosion in the temperature range of 273.15 K-2273.15 K.

3) The calculation results of density of states show that the interaction between the 5f orbital of plutonium atom and the orbitals of two nitrogen atoms has made an important contribution to the formation of Pu-N bond. The energy region in which the interaction promotes bonding is generally smaller than the energy at HOMO, while in the energy region where the energy is larger than that at HOMO, the interaction between them is generally unfavorable to the formation of Pu-N bond.

4) The results of AIM analysis give us a quantitative understanding of the properties of bcps in each structure in the two reaction pathways, and show more clearly the changes of electronic properties during the breaking of N-N bond and the formation of Pu-N bond. From the results of ELF analysis, the evolution process of bonds can be investigated more comprehensively. It is worth noting that the two analytical methods have reached the same conclusion, that is, the proximity of plutonium atoms to nitrogen molecules will activate and break its N-N bond, and then the separated nitrogen atoms will bond with plutonium atoms. In addition, we can also see that it is easier to activate the N-N bond when the plutonium atom approaches the nitrogen molecule from the direction perpendicular to the N-N bond than from one end of the nitrogen molecule.

Funding

All the research costs are supported by postgraduate funds from the PLA Rocket Force University of Engineering.

Conflicts of interest

All the authors have no conflict of interests.

Availability of data and material

All the data and material involved in this paper are true, reliable and available.

Code availability

All the work is performed on TianHe-2 platform, Lvliang Cloud Computing Centre of China. Gaussian16 software is used to search the chemical reaction path and optimize each structure. The thermodynamic and dynamic analysis is completed by using the Multiwfn program, and all the programs and codes are available.

Authors' contributions

The work of calculation and paper writing was done by Zhao-Yang Zhao, and the analysis of the results was done by Zhao-Yang Zhao and Guo-Liang Wang. During this period, Chun-Bao Qi, Xu-Dan Chen and Xin-Li Sun provided valuable guidance.

References

1. Heaven MC (2006) Probing actinide electronic structure using fluorescence and multi-photon ionization spectroscopy. Physical Chemistry Chemical Physics 8 (39):4497-4509

2. Goncharov V, Heaven MC (2006) Spectroscopy of the ground and low-lying excited states of ThO^+. The Journal of chemical physics 124 (6):064312

3. Gibson JK, Haire RG, Santos M, Marçalo J, Pires de Matos A (2005) Oxidation studies of dipositive actinide ions, An^{2+} (An= Th, U, Np, Pu, Am) in the gas phase: Synthesis and characterization of the isolated uranyl, neptunyl, and plutonyl ions UO_2^{2+} (g), NpO_2^{2+} (g), and PuO_2^{2+} (g). The Journal of Physical Chemistry A 109 (12):2768-2781

4. Cox RM, Armentrout P, de Jong WA (2015) Activation of CH4 by Th+ as studied by guided ion beam mass spectrometry and quantum chemistry. Inorganic Chemistry 54 (7):3584-3599

5. Heaven MC, Barker BJ, Antonov IO (2014) Spectroscopy and structure of the simplest actinide bonds. The Journal of Physical Chemistry A 118 (46):10867-10881

6. Cox RM, Armentrout P, de Jong WA (2016) Reactions of Th++ H_2, D_2, and HD studied by guided ion beam tandem mass spectrometry and quantum chemical calculations. The Journal of Physical Chemistry B 120 (8):1601-1614

7. Pereira CC, Marsden CJ, Marçalo J, Gibson JK (2011) Actinide sulfides in the gas phase: experimental and theoretical studies of the thermochemistry of AnS (An= Ac, Th, Pa, U, Np, Pu, Am and Cm). Physical chemistry chemical physics 13 (28):12940-12958

8. Shim J, Haule K, Kotliar G (2007) Fluctuating valence in a correlated solid and the anomalous properties of δ-plutonium. Nature 446 (7135):513-516

9. Hecker SS (2001) The complex world of plutonium science. MRS Bulletin 26 (9):672-678

10. Wirth BD, Schwartz AJ, Fluss MJ, Caturla MJ, Wall MA, Wolfer WG (2001) Fundamental studies of plutonium aging. MRS Bulletin 26 (9):679-683

11. Luo W, Wang Q, Wang X, Gao T (2019) The plutonium chemistry of Pu+ O 2 system: the theoretical investigation of the plutonium–oxygen interaction. Journal of the Iranian Chemical Society 16 (6):1157-1162

12. Osborne J (2010) Arguing to learn in science: The role of collaborative, critical discourse. Science 328 (5977):463-466

13. Li P, Niu W, Gao T (2017) Systematic analysis of structural and topological properties: new insights into $PuO_2(H_2O)_n^{2+}$(n= 1–6) complexes in the gas phase. RSC advances 7 (8):4291-4296

14. Haschke JM, Allen TH, Stakebake JL (1996) Reaction kinetics of plutonium with oxygen, water and humid air: Moisture enhancement of the corrosion rate. Journal of Alloys and Compounds 243 (1-2):23-35

15. Haschke JM, Hodges III AE, Bixby GE, Lucas RL (1983) Reaction of plutonium with water kinetic and equilibrium behavior of binary and ternary phases in the Pu+O+H system. Rockwell International Corp., Golden, CO (USA). Rocky Flats Plant,

16. Clark DL, Hobart DE, Michaudon AF, Boring AM, Smith JL, Wills JM, Eriksson O, Arko AJ, Joyce JJ, Cooper BR Sc ence Los Alamos.

17. Atta-Fynn R, Ray AK (2007) Relaxation of the (1 1 1) surface of δ-Pu and effects on atomic adsorption: An ab initio study. Physica B: Condensed Matter 400 (1-2):307-316
18. Becke AD (2005) Real-space post-Hartree–Fock correlation models. The Journal of chemical physics 122 (6):064101
19. Silvi B, Savin A (1994) Classification of chemical bonds based on topological analysis of electron localization functions. Nature 371 (6499):683-686
20. Becke A (2007) The quantum theory of atoms in molecules: from solid state to DNA and drug design. John Wiley & Sons,
21. Bader RF (1985) Atoms in molecules. Accounts of Chemical Research 18 (1):9-15
22. Bader RF, Stephens ME (1975) Spatial localization of the electronic pair and number distributions in molecules. Journal of the American Chemical Society 97 (26):7391-7399
23. Bianchi R, Gervasio G, Marabello D (2000) Experimental electron density analysis of $Mn_2(CO)$ 10: metal− metal and metal− Ligand bond characterization. Inorganic Chemistry 39 (11):2360-2366
24. Frisch M, Trucks G, Schlegel H, Scuseria G, Robb M, Cheeseman J, Scalmani G, Barone V, Mennucci B, Petersson G (2004) Wallingford, CT: Gaussian. Inc Gaussian 3
25. Schmider HL, Becke AD (1998) Optimized density functionals from the extended G2 test set. The Journal of chemical physics 108 (23):9624-9631
26. Yang W, Wu Q (2002) Direct method for optimized effective potentials in density-functional theory. Physical Review Letters 89 (14):143002
27. Wu X, Ray AK (2001) A hybrid density functional cluster study of the bulk and surface electronic structures of plutonium monoxide. Physica B: Condensed Matter 293 (3-4):362-375
28. Cao X, Dolg M (2002) Segmented contraction scheme for small-core lanthanide pseudopotential basis sets. Journal of Molecular Structure: THEOCHEM 581 (1-3):139-147
29. Marcalo J, Gibson JK (2009) Gas-phase energetics of actinide oxides: an assessment of neutral and cationic monoxides and dioxides from thorium to curium. The Journal of Physical Chemistry A 113 (45):12599-12606
30. Gagliardi L, Roos BO, Malmqvist P-Å, Dyke JM (2001) On the electronic structure of the UO_2 molecule. The Journal of Physical Chemistry A 105 (46):10602-10606
31. Wolstenholme DJ, Cameron TS (2006) Comparative Study of Weak Interactions in Molecular Crystals: H− H Bonds vs Hydrogen Bonds. The Journal of Physical Chemistry A 110 (28):8970-8978
32. Duarte DJ, Sosa GL, Peruchena NM (2013) Nature of halogen bonding. A study based on the topological analysis of the Laplacian of the electron charge density and an energy decomposition analysis. Journal of molecular modeling 19 (5):2035-2041
33. Mata I, Alkorta I, Espinosa E, Molins E (2011) Relationships between interaction energy, intermolecular distance and electron density properties in hydrogen bonded complexes under external electric fields. Chemical Physics Letters 507 (1-3):185-189
34. Mata I, Molins E, Alkorta I, Espinosa E (2009) Effect of an external electric field on the dissociation energy and the electron density properties: The case of the hydrogen bonded dimer HF⋯ HF. The Journal of chemical physics 130 (4):044104

35. Jenkins S, Kirk SR, Guevara-García A, Ayers PW, Echegaray E, Toro-Labbe A (2011) The mechanics of charge-shift bonds: A perspective from the electronic stress tensor. Chemical Physics Letters 510 (1-3):18-20

36. Lu T, Chen F (2012) Multiwfn: a multifunctional wavefunction analyzer. Journal of computational chemistry 33 (5):580-592

37. Meana-Paneda R, Truhlar DG, Fernández-Ramos A (2010) Least-action tunneling transmission coefficient for polyatomic reactions. Journal of chemical theory and computation 6 (1):6-17

38. Woese CR (2002) On the evolution of cells. Proceedings of the National Academy of Sciences 99 (13):8742-8747

39. Lu T (2020) Shermo: A general code for calculating molecular thermochemistry properties.

40. De Almeida K, Ramalho T, Neto J, Santiago R, Felicíssimo V, Duarte H (2013) Methane dehydrogenation by niobium ions: a first-principles study of the gas-phase catalytic reactions. Organometallics 32 (4):989-999

41. Farrugia LJ, Evans C, Senn HM, Hänninen MM, Sillanpää R (2012) QTAIM view of metal–metal bonding in di-and trinuclear disulfido carbonyl clusters. Organometallics 31 (7):2559-2570

42. Kraka E, Cremer D, Koller J, Plesničar B (2002) Peculiar structure of the HOOO-anion. Journal of the American Chemical Society 124 (28):8462-8470

43. Cremer D, Kraka E (1984) A description of the chemical bond in terms of local properties of electron density and energy. Croatica Chemica Acta 57 (6):1259-1281

Figures

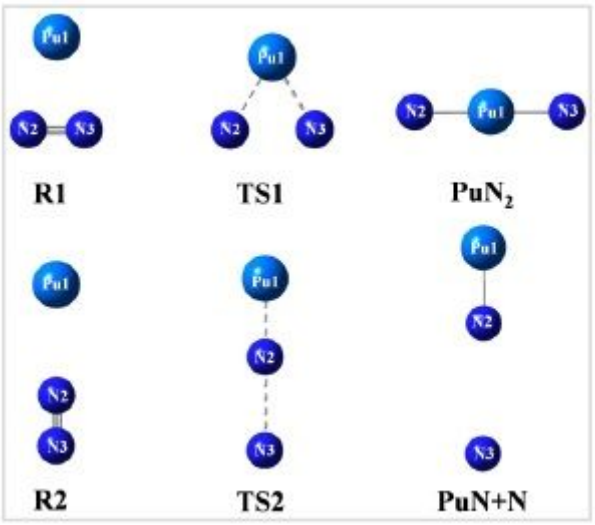

Figure 1

The optimized geometric structure diagram of all intermediates and transition states

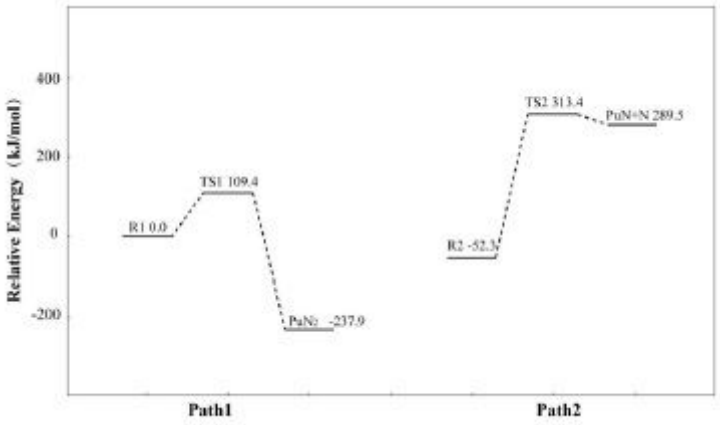

Figure 2

The relative energies of all intermediates and transition states involved in the two reaction pathways composites

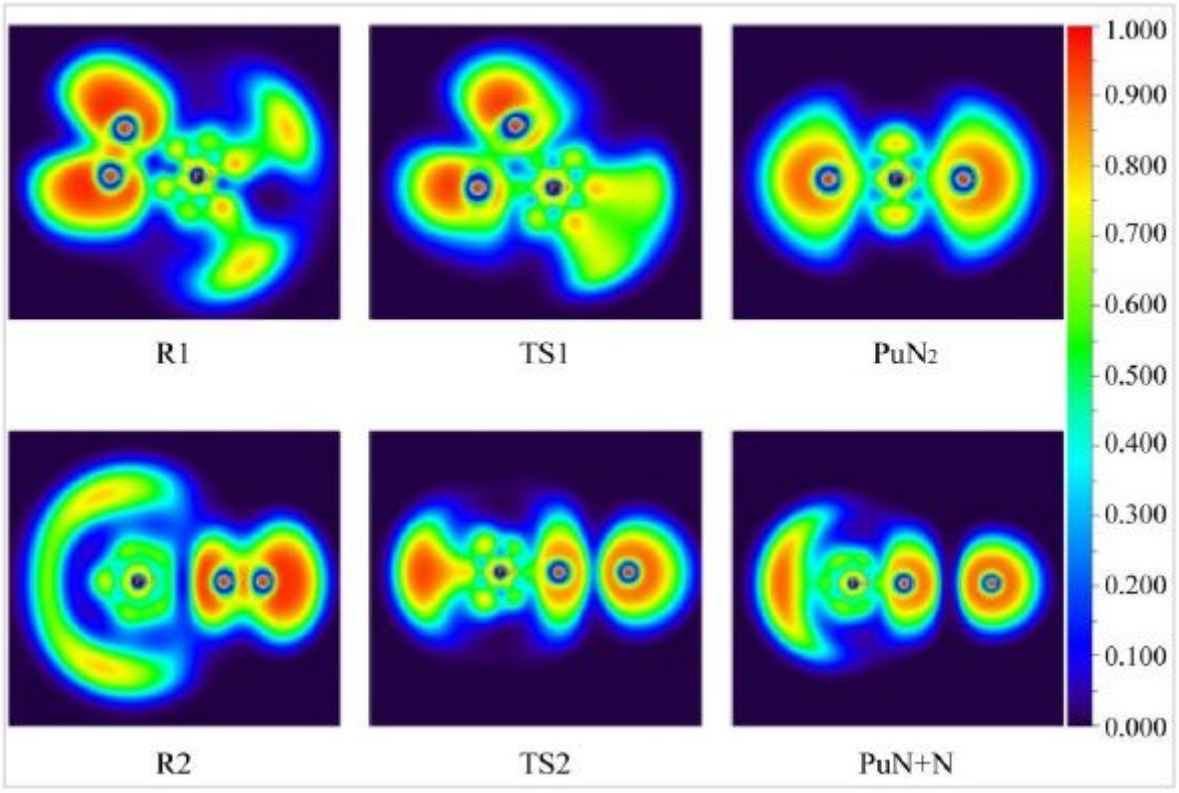

Figure 3

ELF projection map of all intermediates and transition states

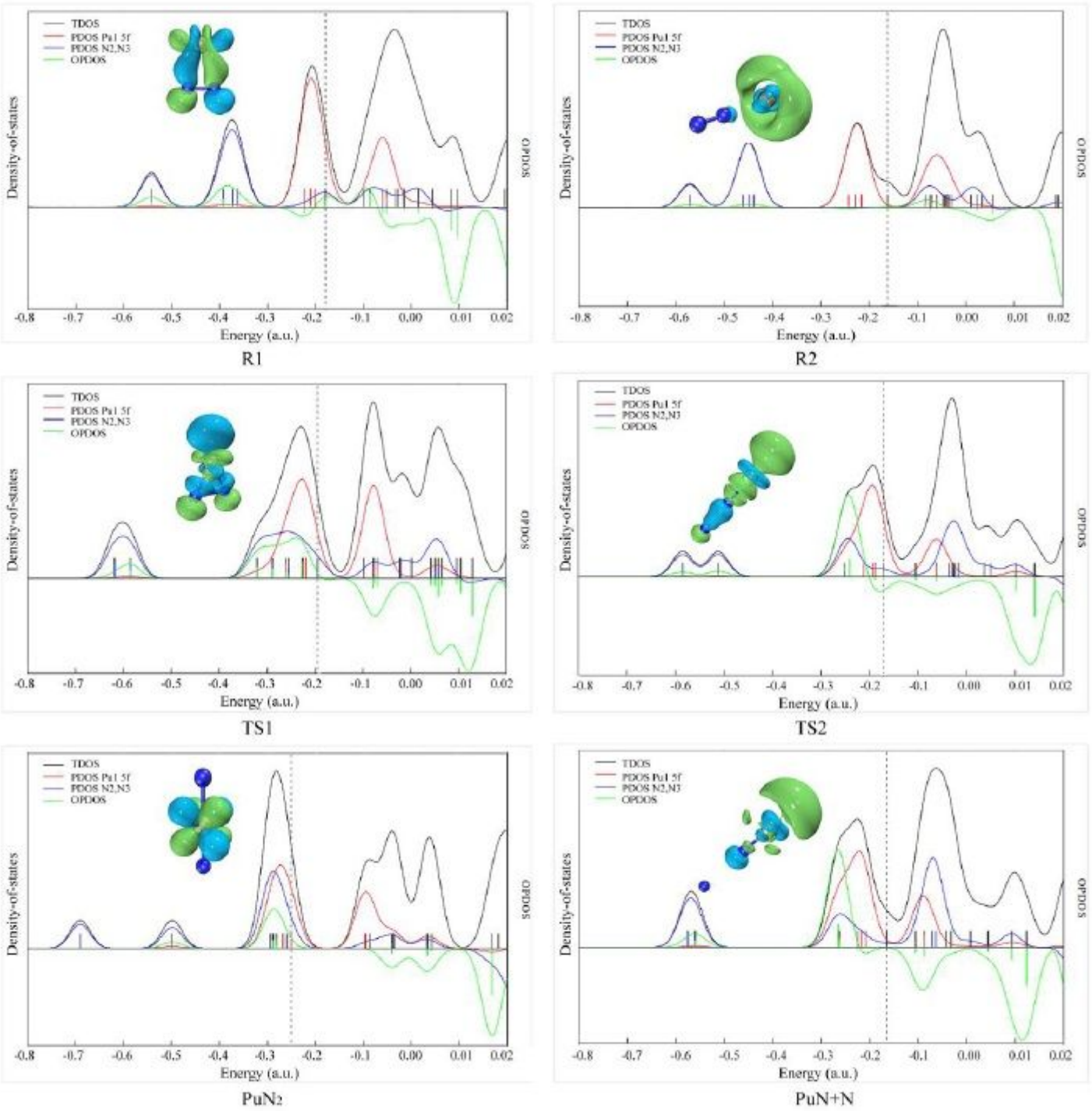

Figure 4

The TDOS, PDOS and OPDOS for all intermediates and transition states.

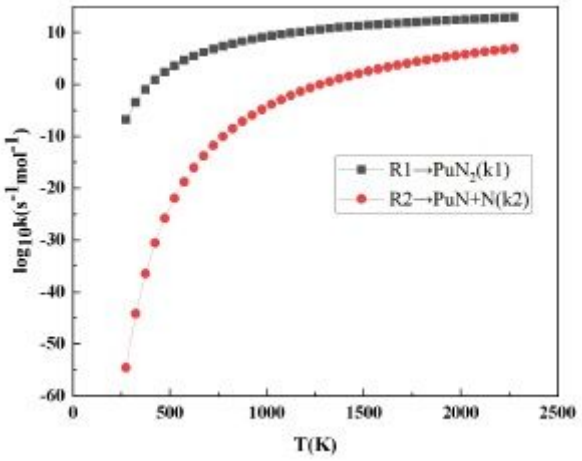

Figure 5

The reaction rate constant (k) of R1：PuN2 and R2：PuN+N in the temperature range of 273.15K- 2273.15K (the pressure is set at 1atm).